Published in final edited form as:
J Immunol. 2009 February 15; 182(4): 2093–2101. doi:10.4049/jimmunol.0802491.

Conditional inactivation of TACE by a *Sox9* promoter leads to osteoporosis and increased granulopoiesis via dysregulation of IL-17 and G-CSF[1]

Keisuke Horiuchi[*,†,2], **Tokuhiro Kimura**[‡], **Takeshi Miyamoto**[†,§], **Kana Miyamoto**[†], **Haruhiko Akiyama**[¶], **Hironari Takaishi**[†], **Hideo Morioka**[†], **Takashi Nakamura**[¶], **Yasunori Okada**[‡], **Carl P. Blobel**[‖], and **Yoshiaki Toyama**[†]

[*] Department of Anti-aging Orthopedic Research, Keio University, School of Medicine, 35 Shinanomachi, Shinjuku-ku, Tokyo 160-8582, Japan

[†] Department of Orthopedic Surgery, Keio University, School of Medicine, 35 Shinanomachi, Shinjuku-ku, Tokyo 160-8582, Japan

[‡] Department of Pathology, Keio University, School of Medicine, 35 Shinanomachi, Shinjuku-ku, Tokyo 160-8582, Japan

[§] Department of Musculoskeletal Reconstruction and Regeneration Surgery, Keio University, School of Medicine, 35 Shinanomachi, Shinjuku-ku, Tokyo 160-8582, Japan

[¶] Department of Orthopedics, Kyoto University, Konoe-cho, Yoshida Sakyo-ku, Kyoto 606-8507, Japan

[‖] Arthritis and Tissue Degeneration Program, Hospital for Special Surgery, Caspary Research Building 541 East 71st Street, New York, NY 10021

Abstract

The TNFα converting enzyme (TACE/ADAM17) is involved in the proteolytic release of the ectodomain of diverse cell surface proteins with critical roles in development, immunity and hematopoiesis. As the perinatal lethality of TACE-deficient mice has prevented an analysis of the roles of TACE in adult animals, we generated mice in which floxed *Tace* alleles were deleted by *Cre* recombinase driven by a *Sox9* promoter. These mutant mice survived up to 9–10 months, but exhibited severe growth retardation as well as skin defects and infertility. The analysis of the skeletal system revealed shorter long bones and prominent bone loss, characterized by an increase in osteoclast and osteoblast activity. In addition, these mice exhibited hypercellularity in the bone marrow and extramedullary hematopoiesis in the spleen and liver. Flow cytometric analysis of the bone marrow cells showed a sharp increase in granulopoiesis and in the population of c-Kit-1^+ Sca-1^+ lineage$^-$ cells, and a decrease in lymphopoiesis. Moreover, we found that serum levels of IL-17 and G-CSF were significantly elevated compared with control littermates. These findings indicate that TACE is associated with a regulation of IL-17 and G-CSF expression in vivo, and

[1]This work was supported by The Uehara Memorial Foundation, The Mochida Memorial Foundation, and Grants-in-aid for Scientific Research from the Ministry of Education, Culture, Sports, Science, and Technology of Japan (19591765) to K.H.

[2]Address correspondence and reprints request to: Dr. Keisuke Horiuchi, the Department of Orthopedic Surgery, Keio University, School of Medicine, 35 Shinanomachi, Shinjuku-ku, Tokyo 160-8582, Japan, Tel: +81-3-5363-3812, FAX: +81-3-3353-6597, horiuchi@z3.keio.jp.

Discloser
The authors have no financial conflict of interest.

that the dysregulation in G-CSF production is causally related to both the osteoporosis-like phenotype and the defects in the hematopoietic system.

Keywords

TACE/ADAM17; granulopoiesis; bone metabolism; G-CSF

Introduction

In order to properly communicate and interact with their surrounding milieu, cells must continuously regulate the expression of cell surface molecules, not only by transcriptional mechanisms but also by post-transcriptional modifications. In recent years, various membrane-bound molecules have been shown to be cleaved and released from the cell surface. The proteolytic release of extracellular domains of membrane-bound proteins, also referred to as “ectodomain shedding”, has emerged as a critical post-translational mechanism for regulating the function and the availability of membrane-bound proteins (1–4).

The TNFα converting enzyme (TACE; also known as ADAM17 (a disintegrin and metalloprotease 17)) [3] was originally identified as a protease responsible for the ectodomain shedding of the membrane-bound precursor of TNFα (5,6). TACE is a type-1 membrane protein and is expressed virtually in all organs in vivo, with high levels of expression in the heart, skeletal muscle, lung, placenta, testis and ovary (5,7). Intriguingly, subsequent studies have revealed TACE as the key regulator for two clinically important signaling pathways; namely, the TNFα-TNF receptor and the epidermal growth factor receptor (EGFR) ligands-EGFR signaling pathways. TNFα is one of the most crucial modulators of the host defense and of the pathogenesis of various inflammatory disorders, such as endotoxin shock, Crohn’s disease, asthma and rheumatoid arthritis (8–11), while EGFR signaling is dysregulated in many cancers and related to their etiology (12–14). Since TACE is essential for membrane-bound pro-TNFα and membrane-bound EGFR ligands to become fully active in vivo, molecular targeting of TACE is deemed beneficial for the treatment of these disorders.

In addition to TNFα and the ligands for EGFR, TACE has also been implicated in the processing of various membrane bound molecules involved in the regulation of the immune system and hematopoietic system. These include the receptors for TNFα, IL-6 receptor, Notch, ICAM-1, VCAM-1, c-Kit ligand, CD44 and cell surface CSF-1, to name a few examples (15–19). Because of the perinatal lethality of *Tace*-deficient mice (20), radiation-chimeric mice reconstituted with *Tace*-deficient bone marrow cells were utilized in several studies to evaluate the functions of TACE in the hematopoietic cells *in vivo* (21,22). However, the consequence of inactivation of TACE in non-hematopoietic cells in adult animals and its potential effects on the hematopoietic system remained poorly understood. In the current study, we took advantage of the *Cre*-LoxP system and generated conditional *Tace*-deficient mice, in which a *Cre* recombinase gene is expressed under the control of a *Sox9* promoter (*Tace*$^{flox/flox}$*; Sox9-Cre*; henceforth referred as *Tace/Sox9*) (10,23). SOX9 is an essential transcription factor for skeletal development and is expressed in all osteo-chondroprogenitor cells as well as in many other organs, including the pancreas, heart, lung, brain and skin, but not in hematopoietic cells (23,24).

[3]The abbreviations used are: TACE, TNF-α converting enzyme; KSL, c-Kit-1^{+} Sca-1^{+} Lineage^{-} sKitL, soluble c-Kit ligand; BrdU, 5-bromodeoxyuridine; EGFR, epidermal growth factor receptor; MPO, myeloperoxidase; vWF, von Willebrand factor.

Herein we describe the phenotypical analysis of *Tace/Sox9* mice, which includes defects in bone metabolism and hematopoiesis, as well as impaired skin development, growth retardation and infertility. Moreover, we found that the serum levels of G-CSF and its major upstream regulator, IL-17, were both significantly increased in *Tace/Sox9* mice compared with control littermates. Since G-CSF is a potent stimulator of both osteoclastogenesis and granulopoiesis, these observations indicate that the dysregulated G-CSF production could be responsible for the osteoporosis-like phenotype and the defects in the hematopoietic system in *Tace/Sox9* mice. The current study thus sheds new light on the roles of TACE in bone metabolism and hematopoiesis.

Materials and Methods

Mice

Generation of $Tace^{flox/flox}$ mice and *Sox9-Cre* knock-in mice was previously described (10,23). $Tace^{flox/flox}$ mice were mated with *Sox9-Cre* knock-in mice to generate $Tace^{flox/+}$/*Sox9-Cre* mice. $Tace^{flox/+}$/*Sox9-Cre*+ mice were viable and fertile, and were further crossed with $Tace^{flox/flox}$ mice to generate *Tace/Sox9* ($Tace^{flox/flox}$/*Sox9-Cre*+) mice. The genotype of the offspring from $Tace^{flox/flox}$ and $Tace^{flox/+}$/*Sox9-Cre* matings at 2 weeks after birth followed a Mendelian distribution pattern (total=166; *Tace/Sox9, 40;* $Tace^{flox/+}$/*Sox9-Cre, 43;* $Tace^{flox/+}$,41; $Tace^{flox/flox}$, 42). CAG-CAT-Z reporter mice were generously provided by Dr. Jun-ichi Miyazaki (Osaka Univ. Medical School) (25). All mice were maintained under a 12 hour light-dark cycle with *ad libitum* access to regular feed and water. The mice were housed in a specific-pathogen free environment and fed with sterile water and feed. All mice used in the current study were of mixed genetic background (129Sv, C57Bl/6), and all comparisons described here were between littermates. All animal experiments were approved by the Institutional Animal Care and Use Committee of the Keio University School of Medicine.

Histology

Tissues were fixed in 4% paraformaldehyde/PBS, sectioned and then stained with hematoxylin and eosin (H&E). For 5-bromodeoxyuridine (BrdU) labeling, BrdU (30 μg/g body weight) was injected intraperitoneally 3 hours prior to sacrificing the animal. Immunostaining was performed using the following antibodies; myeloperoxidase (MPO; DAKO, Glostrup, Denmark), CD3 (Serotec, Kidlington, UK), B220 (eBioscience, San Diego, CA), von Willebrand factor (vWF; DAKO) and BrdU (DAKO). The nuclei were counterstained with methyl green or hematoxylin. The sections were photographed with a DXM1200 camera (Nikon, Tokyo, Japan) on a BX50 microscope (Olympus, Tokyo, Japan). The expression pattern of SOX9 was examined by mating *Sox9-Cre* knock-in mice with CAG-CAT-Z reporter mice (25), which express β-gal upon *Cre*-mediated excision of the loxP-flanked CAT (chloramphenicol acetyltranferase) located between the CAG (cytomegalovirus immediate early enhancer-chicken β-actin hybrid promoter) and the lacZ gene. The tissues taken from newborn or 2 week-old *Sox9-Cre*/CAG-CAT-Z reporter mice and the control mice were whole-mount stained with X-gal (5-bromo-4-chloro-3-indolyl-b-D-galactopyranoside) and were subsequently sectioned.

Western blot analysis

Primary osteoblasts were harvested from the calvaria of newborn *Control* or *Tace/Sox9* mice. Bone marrow macrophages were prepared as described previously (10). In short, bone marrow was collected from the tibiae and femurs of 6-week-old *Tace/Sox9* or littermate *Control* mice. RBCs were removed with RBC lysis buffer (Roche), and the remaining cells were plated on petri dishes. Adherent cells were grown in αMEM with 10% FCS, antibiotics, and 50 ng/ml recombinant mouse macrophage CSF (Wako, Tokyo, Japan) for 4

days and then used as bone marrow macrophages. The cells were lysed with 1% Triton-X/PBS containing protease inhibitor cocktail (Sigma). The sample proteins were separated by SDS-PAGE and Western blots were performed as previously described, using anti-sera against the cytoplasmic domain of TACE (26).

Flow cytometry

Bone marrow cells were isolated by flushing femurs with 5% FCS/PBS, and splenocytes were collected by mechanical disruption of the spleen. The cells were filtered through a cell strainer (BD Falcon) to remove debris. We used the following monoclonal antibodies for flow cytometric analysis: c-Kit (2B8), Sca-1 (E13-161.7), B220 (RA3-6B2), CD3 (SK-7), Gr-1 (RB6-8C5), IL-17, and Mac-1 (M1/70). All the antibodies were from BD Bioscience (Franklin Lakes, NJ). The percentages of $B220^{+}$ $CD3^{-}$ (B lymphocytes) and $B220^{-}$ $CD3^{+}$ (T lymphocytes) in the bone marrow and spleen were determined by direct immunofluorescence using a laser flow cytometer (FACSCalibur system, BD Bioscience). A mixture of monoclonal antibodies against CD4, CD8, B220, TER-119, Mac-1 and Gr-1 was used as a lineage marker (Lineage). For the detection of intracellular IL-17, the spleen cells were fixed and permeabilized using Cytofix/Cytoperm (BD Pharmingen) and were subjected to flow cytometric analysis.

Colony forming assay

Colony forming assays were performed using methylcellulose-based medium (Methocult #03534, StemCell Technologies, Vancouver, Canada) following the manufacturer's instructions. Bone marrow cells (1×10^4/35 mm dish) and spleen cells (1×10^5/35 mm/dish) isolated from 10 week-old mice were incubated for 7 days and the number of the colonies was counted under a light microscope.

Dual X-ray absorptiometry and microcomputed tomography analysis

All microcomputed tomography analysis was carried out using 8 week-old control and *Tace/Sox9* mice littermates. Femurs were excised and fixed with 75% ethanol. Bone mineral density (BMD) of the femurs was measured by Phantom for Bone Mineral Quantity (Kyoto Kagaku, Kyoto, Japan). Two-dimensional images of the distal femurs were obtained by microcomputed tomography scan, Scan Xmate (Comscantecno, Kanagawa, Japan) and the three-dimensional images were reconstructed by 3D software, TRI/3D-BON (Ratoc System Engineering, Tokyo, Japan). Four mice for each group were analyzed.

Histomorphometric analysis

All histomorphometric analysis was carried out using 8 week-old control and *Tace/Sox9* mice littermates. Femurs were excised, fixed with 75% ethanol, embedded in glycolmethacrylate resin, and sectioned in 3 μm slices. For double labeling, mice were injected subcutaneously with calcein (8 mg/kg body weight) at 4 days and 1 day before sacrifice. The sections were stained with toluidine blue and were subjected to histomorphometric analyses under a light microscope with a micrometer, using a semiautomated image analyzer (Osteoplan II, Carl Zeiss, Thornwood, NY). Parameters for the trabecular bone were measured in an area 1.62–2.34 mm^2 in size from 1.2 mm above the growth plate at the distal metaphysis. Four mice for each group were analyzed.

Determination of cytokine levels

The serum levels of IL-17, IL-23, G-CSF, soluble c-Kit ligand (sKitL) and SDF-1 were measured by sandwich ELISA (Quantikine, R & D Systems, Minneapolis, MN) following the manufacturer's instructions. Preparation of bone marrow extracellular extracts was performed as previously described (27). In short, the bone marrow was directly flushed into

500 μl PBS containing protease inhibitors. The cells were pelleted at 400g, 4°C for 5 minutes. Supernatants containing bone marrow fluids were taken and stored at −80°C until further analysis.

Statistical analysis

All data are presented as mean ± s.d. Student's *t*-test for two samples assuming equal variances were used to calculate the P-values. P-values smaller than 0.05 were considered statistically significant.

Results

Tace/Sox9 mice exhibit skin defects and growth retardation but survive into adulthood

In order to analyze the functions of TACE in non-hematopoietic cells, we crossed $Tace^{flox/flox}$ mice with *Sox9-Cre* knock-in mice, in which a *Cre* recombinase gene preceded by an internal ribosome entry site was inserted into the 3′ untranslated region of the *Sox9* gene (23). SOX9 is expressed in a relatively wide range of tissues, including bone, cartilage, skin, lung, pancreas, digestive tract, brain and kidney as previously described (Fig. 1A) (23,28,29). On the other hand, very limited expression was seen in the spleen and thymus, indicating that hematopoietic cells do not detectably express SOX9 at any stage of differentiation. Western blot analysis of primary osteoblasts from calvaria showed a nearly complete lack of TACE in the osteoblasts, whereas no significant change in the expression of TACE was seen in the bone-marrow derived macrophages (Fig. 1B). *Tace/Sox9* mice were born with open eyes and were indistinguishable from the previously described $Tace^{\delta Zn/\delta Zn}$ mice and $Tace^{-/-}$ mice (data not shown) (10,20). However, in contrast to $Tace^{\delta Zn/\delta Zn}$ mice and $Tace^{-/-}$ mice, which have thickened and misshapen aortic, pulmonic and tricuspid valves (10,30), there was no evident defects in these heart valves in *Tace/*Sox9 mice (data not shown), even though SOX9 is expressed in the endocardial cushion and the valves (Fig. 1A) (28). None of the other genotypes ($Tace^{flox/+}$*/Sox9-Cre*, $Tace^{flox/+}$ or $Tace^{flox/flox}$, henceforth referred to as *Control*) showed any evident phenotype or histological defects (data not shown). *Tace/Sox9* mice showed growth retardation with skin and hair defects similar to those seen in $Egfr^{-/-}$ mice (Fig. 1C) (31–33), but unlike $Egfr^{-/-}$ or $Tace^{-/-}$ mice, the majority of *Tace/Sox9* mice survived longer than 5 months (Fig. 1D). The reason(s) for their death after 5 months is not clear at present. A difference in the body weight became evident after 12 weeks of age (Fig. 1E); whereas the average weight of *Tace/Sox9* mice was only up to 15% below that of *Control* animals until 8 weeks of age. Additionally, female *Tace/Sox9* mice were sterile and the fertility of male *Tace/Sox9* mice was severely impaired (data not shown).

Tace/Sox9 mice exhibit shorter long bones and an osteoporosis-like phenotype

Histological analysis revealed an elongated hypertrophic zone and a shorter proliferating zone in the bones of *Tace/Sox9* mice compared to those of *Control* mice (Fig. 2A). The elongation of the growth plates was prominent at 2–3 weeks of age, and became less evident in older mice. Unexpectedly, we found that the bone marrow of *Tace/Sox9* mice was not replaced with adipose tissue but remained filled with bone marrow cells (Fig. 2A). The bone marrow of metatarsi in *Control* mice became replaced with adipocytes at around 3 weeks of age and was almost completely filled with fat cells by 8 weeks after birth; however the bone marrow of *Tace/Sox9* mice remained filled with bone marrow cells at least up to 4 months after birth (data not shown). These observations indicated a possible defect in the hematopoietic system in *Tace/Sox9* mice.

When DNA synthesis of the growth plate cells was evaluated by BrdU incorporation, there was a significant decrease in the number of BrdU-incorporated cells in *Tace/Sox9* mice (Fig.

2B). X-ray analysis revealed no overt abnormalities in the skeletal system; however the femur length of *Tace/Sox9* mice was 10–15 % shorter and the bone mass was decreased compared to that of *Control* (Fig. 2C). On the other hand, there was no change in the growth rate of primary chondroblasts from rib cartilage or calvarial osteoblasts in vitro, indicating that impaired growth of chondroblasts in vivo was caused by a cell-extrinsic mechanism (data not shown).

To further examine the bone defects found in X-ray analysis, we prepared sections from 8, 16 and 24 week-old mice for histological evaluation. van Gieson-stained sections of distal femurs of *Tace/Sox9* mice revealed prominent bone loss, which was manifested by less trabecular bone and thinner cortical bone (Fig. 3A). This phenotype was already evident at 8 weeks and then progressively worsened. Microcomputed tomography analysis confirmed these observations (Fig. 3B and C). Histomorphometric analysis revealed that both osteoclasts-related parameters (eroded surfaces (ES/BS), osteoclast numbers (N.Oc/B.Pm) and osteoclast surfaces (Oc.S/BS)) and osteoblasts-related parameters (osteoid volume (OV/BV), osteoid surfaces (OS/BS), and osteoblast surfaces (Ob.S/BS)) were increased in *Tace/Sox9* mice compared with *Control*; on the other hand, the mineral apposition rate (MAR) and bone formation rate (BFR/BS) were not altered. These data show that inactivation of TACE under the control of a *Sox9* promoter results in two different bone defects; 1) elongation in growth plate and shorter long bones (0–8 weeks after birth), and 2) high-turnover type osteoporosis characterized by increased activities in both osteoblasts and osteoclasts (approximately 8 weeks after birth).

Splenomegaly and dysregulated lymphopoiesis and granulopoiesis in Tace/Sox9 mice

In addition to the hypercellularity found in the bone marrow (Fig. 2A), *Tace/Sox9* mice had a proportionally larger spleen than in *Control* mice (Fig. 4A). These observations led us to assess potential defects in the hematopoietic system. Flow cytometric analysis of the bone marrow cells and spleen cells from 8 week-old *Tace/Sox9* mice revealed a relative decrease in the population of B lymphocytes ($CD3^{-}$ $B220^{+}$) and T lymphocytes ($CD3^{+}$ $B220^{-}$) and an increase in the population of Mac-1^{+}Gr-1^{+} cells (which includes monocytes/macrophages and neutrophils) compared to those of *Control* mice (Fig. 4B and C). There was an absolute lymphopenia in the bone marrow; however the number of lymphocytes in the spleen was comparable in *Tace/Sox9* and *Control* mice. On the other hand, no apparent difference in these cell populations was observed in the thymus (data not shown).

Since the soluble form of TNFα is essential for the development of the lymphoid pulps in the spleen (34), we examined whether this structure was affected in *Tace/Sox9* mice. The spleen sections were immunostained with B220 (a B lymphocyte marker) and with CD3 (a T lymphocyte marker). The lymphocytes (B220-positive cells and CD3-positive cells) were fewer and the formation of lymphoid pulps was less mature at 3 weeks of age compared to *Control* mice, indicating that the development of lymphoid follicles was retarded, but not disturbed, at this stage. On the other hand, splenomegaly was not evident at this stage of splenic development (Fig. 4D). In 8 week-old *Tace/Sox9* mice, lymphoid follicles had developed to a comparable stage as in *Control* mice, but an expansion of the red pulp of the spleen led to splenomegaly (Fig. 4E). The thymus was transiently smaller in *Tace/Sox9* mice at around 3 weeks of age compared to *Control*; however it developed to a comparable level by 8 weeks after birth without any apparent histological abnormalities (data not shown). These results suggest that a TACE-deficient environment results in the dysregulation of lymphoid development and granulopoiesis.

Extramedullary hematopoiesis and increase in KSL cell population are observed in adult Tace/Sox9 mice

Consistent with the results of flow cytometric analysis, histology of the spleen in 8 week-old *Tace/Sox9* mice revealed an increase in the number of granulocytic cells of various differentiation stages, and also megakaryocytes in the red pulp (Fig. 5A). Immunostaining with MPO (a marker for myeloid cells) and vWF (a marker for megakaryocytes) confirmed these observations (Fig. 5B). Thus the enlargement of the spleen in *Tace/Sox9* mice was caused by the expansion of the red pulp filled primarily with proliferating granulocytic cells. Moreover, MPO-positive cells and vWF-positive cells were also present in the liver of *Tace/Sox9* mice, indicating the presence of extramedullary hematopoiesis in this organ as well (Fig. 5C). The degree of extramedullary hematopoiesis in the liver became more prominent as these mutant mice became older (data not shown). To assess whether the population of hematopoietic stem cells was also affected in *Tace/Sox9* mice, we analyzed the population of KSL cells in bone marrow, which is enriched in hematopoietic stem cells (35). As shown in Fig. 5D, the population of KSL cells was approximately 3 times higher in the bone morrow of *Tace/Sox9* mice compared to that of *Control* mice. Consistent with these findings, the number of colony forming units (CFU-GM) in the bone marrow and spleen was significantly higher in *Tace/Sox9* mice than in *Control* mice (Fig. 5E). Analysis of complete blood counts revealed a slight, yet statistically significant, increase in the number of white blood cells and platelets, and a decrease in hemoglobulin levels and hematocrit (Fig. 5F). These observations suggest that cell-extrinsic inactivation of TACE led to a significant increase in granulopoiesis which ultimately resulted in extramedullary hematopoiesis in the spleen and liver.

Serum G-CSF and IL-17 levels are highly elevated in Tace/Sox9 mice

The phenotypical analysis described above revealed that lack of TACE activity under the control of a *Sox9* promoter in vivo resulted in high-turnover type osteoporosis, upregulation in granulopoiesis and extramedullary hematopoiesis in adult animals. We next sought to answer whether there could be a common cell-extrinsic factor that could perhaps be responsible for the apparently unrelated hematopoietic and bone defects. Various cytokines and growth factors have been shown to be involved in granulopoiesis and in bone metabolism (36–39). Among these, G-CSF is considered to be the principal cytokine controlling granulocyte development and functions. Moreover, it has been shown that G-CSF enhances the development of osteoclasts and their activity both in vivo and in vitro (40,41). Therefore, G-CSF has dual roles as a modulator for both bone metabolism and hematopoiesis. Based on these observations, we hypothesized that dysregulation in G-CSF production might be involved in the increased granulopoiesis and bone loss observed in *Tace/Sox9* mice. As shown in Fig. 6A, there was a notable increase (approximately 13 fold) in the G-CSF levels in *Tace/Sox9* mice (2639 ± 299 pg/ml) compared with *Control* mice (192 ± 124 pg/ml). Moreover, in line with the notion that G-CSF induces stem cell mobilization via down-regulation of SDF-1 in bone marrow (42,43), the SDF-1 levels in bone marrow extracellular extracts were significantly lower in *Tace/Sox9* mice (0.21 ± 0.10 ng/ml) compared with *Control* (0.34 ± 0.06 ng/ml), while the serum SDF-1 levels remained unaltered (Fig. 6B). The serum sKitL levels were also lower in *Tace/Sox9* mice (69.8 ± 13.1 pg/ml) compared with *Control* mice (130.9 ± 29.4 pg/ml) (Fig. 6C), even though the release of c-Kit ligand into serum has been shown to be upregulated by an administration of G-CSF (44).

Several lines of evidence have revealed IL-17 as an important upstream regulator of G-CSF in vivo (45–48). IL-17 is a pro-inflammatory cytokine produced by multiple cell types, including $CD4^+$ αβ T cells, γδ T cells, NK cells, and neutrophils, and induces granulopoiesis via induction of G-CSF. Furthermore, IL-17 can also indirectly upregulate

osteoclastogenesis (49). To assess a possible involvement of IL-17, we examined the serum IL-17 levels and found that they were significantly elevated in *Tace/Sox9* mice compared to *Control* mice(Fig. 6D; *Control*, <5 pg/ml; *Tace/Sox9*, 231 ± 123 pg/ml). Given these observations, we next examined whether the population of IL-17 producing cells was affected in *Tace/Sox9* mice, and found that there was an increase in the number of IL-17 producing cells in *Tace/Sox9* spleen compared with that in *Control* animals (Fig. 6E). Of note, most of these cells were negative for CD4, indicating that this cell population predominantly consisted of γδ T cells and/or NK cells. Taken together, these results indicate that a TACE-deficient environment led to a dysregulation of the IL-17/G-CSF axis and that the marked increase in the serum levels of these cytokines was most likely related to the hematopoietic defects and osteoporosis-like phenotype observed in *Tace/Sox9* mice.

Discussion

Currently, there are few studies describing the functions of TACE in adult animals, primarily due to the perinatal lethality of *Tace*$^{-/-}$ mice. The *Tace/Sox9* mice presented in the current study are unique in that, even with various anomalies in a wide range of organs, most survived to adulthood with little variance in the phenotype among the individual mutant mice. Thus, *Tace/Sox9* mice may be very highly useful tools for the analysis of the functions of TACE in vivo. Most importantly, since SOX9 is not expressed in hematopoietic cells and TACE should therefore not be inactivated in lymphocytes or monocytes in *Tace/Sox9* mice, the hematopoietic defects are most likely not caused by a cell-autonomous lack of TACE activity in hematopoietic cells.

The defects in the growth plate and the decreased size of long bones observed in *Tace/Sox9* mice highly resemble those seen in *Egfr*$^{-/-}$ mice and the mice humanized for EGFR (which have almost complete loss of EGFR expression in the bone cells) (50). Therefore, impaired EGFR signaling in the developing bone appears to be causally related to these defects. Previous studies have shown that at least five EGFR ligands (heparin-binding EGF-like growth factor, amphiregulin, TGFα, epiregulin and epigen) can be shed by TACE (7,51,52), and that loss of TACE in vivo usually results in loss of functional activation of these EGFR ligands. However, since bone defects resembling those in *Egfr*$^{-/-}$ or *Tace/Sox9* mice have not yet been reported in mice lacking any of the EGFR-ligands, multiple EGFR ligands or other unidentified substrates of TACE may also be involved in this phenotype. On the other hand, the current study suggests that dysregulation of IL-17 and G-CSF production in *Tace/Sox9* mice is, at least in part, responsible for the osteoporosis-like phenotype and hematopoietic defects observed in *Tace/Sox9* mice

Since TACE is usually involved in the processing of membrane-bound molecules (1–4), the dysregulation of IL-17 and G-CSF production in *Tace/Sox9* mice was an unexpected result. Macrophages and osteoclasts, but not osteoblasts, express the G-CSF receptor, and an administration of G-CSF leads to increased osteoclast numbers in vivo and in vitro culture system (40). The receptor for IL-17 is expressed on osteoblasts, and it has been shown that IL-17 indirectly stimulates bone resorption through the induction of receptor activator of NF-κB ligand, a membrane bound protein which is expressed on osteoblasts and essential for osteoclastogenesis (49). These observations suggest that the osteoporosis-like phenotype and the increase in osteoclast activity observed in *Tace/Sox9* mice are likely caused by the increased serum levels of IL-17 and G-CSF. Consistent with this interpretation, human G-CSF transgenic mice, which produce high levels of human G-CSF (approximately, 1000 pg/ml) in sera, not only exhibit hematopoietic defects (including granulocytosis, extramedullary hematopoiesis and increase in hematopoietic stem cell population), but also develop osteoporosis with increased osteoclast activity (41,53,54). Since the serum G-CSF levels were even higher in *Tace/Sox9* mice (2639 ± 299 pg/ml) compared with that in human G-

CSF transgenic mice, it would be reasonable to assume that the defects in both bone metabolism (increased osteoclast activity and loss of bone mass) and hematopoiesis were primarily caused by the elevated G-CSF production. Nevertheless, further studies will be required to confirm the relation between these defects and the dysregulation of IL-17 and G-CSF expression observed in *Tace/Sox9* mice.

Recent studies have revealed a regulatory model involved in neutrophil homeostasis and cytokine production (45,47). The proposed model suggests that secretion of IL-23 from macrophages and dendritic cells is suppressed by phagocytosis of apoptotic neutrophils, which in turn reduces the production of IL-17 and G-CSF, and ultimately down-regulates granulopoiesis. In the case for leukocyte adhesion molecule-deficient animals, such as $Cd18^{-/-}$ mice (45,47), the neutrophils are unable to efficiently transmigrate into critical peripheral tissues, and therefore macrophages and dendritic cells cannot phagocyte apoptotic neutrophils. Consequently these cells continue to produce IL-23, which in turn results in an increased granulopoiesis via IL-17 and G-CSF. Along these lines, a concomitant increase in serum G-CSF and in IL-17 levels in *Tace/Sox9* mice was found. However, any increase in serum IL-23 was minor compared to the substantial increase in IL-17 and G-CSF levels (the serum IL-23 levels were above the detection limit (>2.28 pg/ml; according to the manufacturer's instructions) only in one out of 9 *Control* mice (3.9 pg/ml), whereas they were detectable in 6 out of 7 *Tace/Sox9* mice (average, 5.8 pg/ml)). Furthermore, a single injection of IL-17 neutralizing antibody into *Tace/Sox9* mice did not significantly affect the serum G-CSF levels (data not shown). Therefore, although we cannot rule out possible involvements of insufficient neutrophil transmigration or defective phagocytosis by macrophages and dendritic cells in *Tace/Sox9* mice, it is more likely that a TACE-deficient environment directly or indirectly leads to the increased production of IL-17 and G-CSF. The link between the elevation of serum IL-17, G-CSF and the lack of TACE-in Sox9-expressing cells remains to be determined.

Processing of membrane-bound c-Kit ligand by MMP-9 and/or Cathepsin K and the increase in the plasma sKitL have been shown to increase mobilization of mediate bone marrow progenitors (43,44). However, we found that the serum levels of sKitL were significantly lower in *Tace/Sox9* mice, suggesting that release of sKitL may not be absolutely required for G-CSF induced stem cell mobilization (55,56). Since the membrane bound c-Kit ligand has indispensible roles in hematopoiesis, as highlighted by the impaired development of hematopoietic cells in the mice with Steel-Dickie mutation, in which only a soluble truncated c-Kit ligand is encoded (57), it is possible that altered processing of c-Kit ligand in the hematopoietic niche in *Tace/Sox9* mice may also have contributed to the dysregulation of KSL cells population. Nevertheless, the current study further corroborates TACE as the major sheddase for membrane bound c-Kit ligand (17).

In conclusion, the current study revealed an unexpected role for TACE in the modulation of bone metabolism and hematopoiesis in vivo. Our data show that conditional inactivation of TACE under the control of a *Sox9* promoter led to a dysregulation in IL-17 and G-CSF production, which ultimately resulted in diverse defects in both bone metabolism and hematopoiesis in adult animals, thereby providing the first evidence for a role of TACE in the regulation of IL-17/G-CSF. Since IL-17or G-CSF is apparently not a direct target molecule for TACE, further investigations will be necessary to elucidate the causal link between TACE-deficient environment and the increase in IL-17 production. Nevertheless, a wide variety of defects and the early death in *Tace/Sox9* mice unequivocally demonstrate indispensible roles of TACE in normal bone growth and adult homeostasis.

Acknowledgments

We thank Dr. Jun-ichi Miyazaki for providing CAG-CAT-Z reporter mice, and Ms. Yuko Hashimoto and Ms. Shizue Tomita for their excellent technical assistance.

References

1. Schlondorff J, Blobel CP. Metalloprotease-disintegrins: modular proteins capable of promoting cell-cell interactions and triggering signals by protein-ectodomain shedding. J Cell Sci 1999;112:3603–3617. [PubMed: 10523497]
2. Blobel CP. ADAMs: key components in EGFR signalling and development. Nat Rev Mol Cell Biol 2005;6:32–43. [PubMed: 15688065]
3. Seals DF, Courtneidge SA. The ADAMs family of metalloproteases: multidomain proteins with multiple functions. Genes Dev 2003;17:7–30. [PubMed: 12514095]
4. Kheradmand F, Werb Z. Shedding light on sheddases: role in growth and development. Bioessays 2002;24:8–12. [PubMed: 11782944]
5. Black RA, Rauch CT, Kozlosky CJ, Peschon JJ, Slack JL, Wolfson MF, Castner BJ, Stocking KL, Reddy P, Srinivasan S, Nelson N, Boiani N, Schooley KA, Gerhart M, Davis R, Fitzner JN, Johnson RS, Paxton RJ, March CJ, Cerretti DP. A metalloproteinase disintegrin that releases tumour-necrosis factor-alpha from cells. Nature 1997;385:729–733. [PubMed: 9034190]
6. Moss ML, Jin SL, Milla ME, Bickett DM, Burkhart W, Carter HL, Chen WJ, Clay WC, Didsbury JR, Hassler D, Hoffman CR, Kost TA, Lambert MH, Leesnitzer MA, McCauley P, McGeehan G, Mitchell J, Moyer M, Pahel G, Rocque W, Overton LK, Schoenen F, Seaton T, Su JL, Becherer JD. Cloning of a disintegrin metalloproteinase that processes precursor tumour-necrosis factor-alpha. Nature 1997;385:733–736. [PubMed: 9034191]
7. Sahin U, Weskamp G, Kelly K, Zhou HM, Higashiyama S, Peschon J, Hartmann D, Saftig P, Blobel CP. Distinct roles for ADAM10 and ADAM17 in ectodomain shedding of six EGFR ligands. J Cell Biol 2004;164:769–779. [PubMed: 14993236]
8. Berry MA, Hargadon B, Shelley M, Parker D, Shaw DE, Green RH, Bradding P, Brightling CE, Wardlaw AJ, Pavord ID. Evidence of a role of tumor necrosis factor alpha in refractory asthma. N Engl J Med 2006;354:697–708. [PubMed: 16481637]
9. Hehlgans T, Pfeffer K. The intriguing biology of the tumour necrosis factor/tumour necrosis factor receptor superfamily: players, rules and the games. Immunology 2005;115:1–20. [PubMed: 15819693]
10. Horiuchi K, Kimura T, Miyamoto T, Takaishi H, Okada Y, Toyama Y, Blobel CP. TNFalpha-converting enzyme (TACE/ADAM17) inactivation in mouse myeloid cells prevents lethality from endotoxin shock. J Immunol 2007;179:2686–2689. [PubMed: 17709479]
11. Scott DL, Kingsley GH. Tumor necrosis factor inhibitors for rheumatoid arthritis. N Engl J Med 2006;355:704–712. [PubMed: 16914706]
12. Fridman JS, Caulder E, Hansbury M, Liu X, Yang G, Wang Q, Lo Y, Zhou BB, Pan M, Thomas SM, Grandis JR, Zhuo J, Yao W, Newton RC, Friedman SM, Scherle PA, Vaddi K. Selective inhibition of ADAM metalloproteases as a novel approach for modulating ErbB pathways in cancer. Clin Cancer Res 2007;13:1892–1902. [PubMed: 17363546]
13. Kenny PA, Bissell MJ. Targeting TACE-dependent EGFR ligand shedding in breast cancer. J Clin Invest 2007;117:337–345. [PubMed: 17218988]
14. Merchant NB, Voskresensky I, Rogers CM, Lafleur B, Dempsey PJ, Graves-Deal R, Revetta F, Foutch AC, Rothenberg ML, Washington MK, Coffey RJ. TACE/ADAM-17: A component of the epidermal growth factor eeceptor axis and a promising therapeutic target in colorectal cancer. Clin Cancer Res 2008;14:1182–1191. [PubMed: 18281553]
15. Murphy G, Murthy A, Khokha R. Clipping, shedding and RIPping keep immunity on cue. Trends Immunol 2008;29:75–82. [PubMed: 18182322]
16. Horiuchi K, Miyamoto T, Takaishi H, Hakozaki A, Kosaki N, Miyauchi Y, Furukawa M, Takito J, Kaneko H, Matsuzaki K, Morioka H, Blobel CP, Toyama Y. Cell surface colony-stimulating factor 1 can be cleaved by TNF-alpha converting enzyme or endocytosed in a clathrin-dependent manner. J Immunol 2007;179:6715–6724. [PubMed: 17982061]

17. Kawaguchi N, Horiuchi K, Becherer JD, Toyama Y, Besmer P, Blobel CP. Different ADAMs have distinct influences on Kit ligand processing: phorbol-ester-stimulated ectodomain shedding of Kitl1 by ADAM17 is reduced by ADAM19. J Cell Sci 2007;120:943–952. [PubMed: 17344430]
18. Nagano O, Murakami D, Hartmann D, De Strooper B, Saftig P, Iwatsubo T, Nakajima M, Shinohara M, Saya H. Cell-matrix interaction via CD44 is independently regulated by different metalloproteinases activated in response to extracellular Ca(2+) influx and PKC activation. J Cell Biol 2004;165:893–902. [PubMed: 15197174]
19. Levine SJ. Mechanisms of soluble cytokine receptor generation. J Immunol 2004;173:5343–5348. [PubMed: 15494479]
20. Peschon JJ, Slack JL, Reddy P, Stocking KL, Sunnarborg SW, Lee DC, Russell WE, Castner BJ, Johnson RS, Fitzner JN, Boyce RW, Nelson N, Kozlosky CJ, Wolfson MF, Rauch CT, Cerretti DP, Paxton RJ, March CJ, Black RA. An essential role for ectodomain shedding in mammalian development. Science 1998;282:1281–1284. [PubMed: 9812885]
21. Li N, Boyd K, Dempsey PJ, Vignali DA. Non-cell autonomous expression of TNF-alpha-converting enzyme ADAM17 is required for normal lymphocyte development. J Immunol 2007;178:4214–4221. [PubMed: 17371977]
22. Li Y, Brazzell J, Herrera A, Walcheck B. ADAM17 deficiency by mature neutrophils has differential effects on L-selectin shedding. Blood 2006;108:2275–2279. [PubMed: 16735599]
23. Akiyama H, Kim JE, Nakashima K, Balmes G, Iwai N, Deng JM, Zhang Z, Martin JF, Behringer RR, Nakamura T, de Crombrugghe B. Osteo-chondroprogenitor cells are derived from Sox9 expressing precursors. Proc Natl Acad Sci U S A 2005;102:14665–14670. [PubMed: 16203988]
24. Akiyama H, Chaboissier MC, Martin JF, Schedl A, de Crombrugghe B. The transcription factor Sox9 has essential roles in successive steps of the chondrocyte differentiation pathway and is required for expression of Sox5 and Sox6. Genes Dev 2002;16:2813–2828. [PubMed: 12414734]
25. Sakai K, Miyazaki J. A transgenic mouse line that retains Cre recombinase activity in mature oocytes irrespective of the cre transgene transmission. Biochem Biophys Res Commun 1997;237:318–324. [PubMed: 9268708]
26. Schlondorff J, Becherer JD, Blobel CP. Intracellular maturation and localization of the tumour necrosis factor alpha convertase (TACE). Biochem J 2000;347:131–138. [PubMed: 10727411]
27. Levesque JP, Takamatsu Y, Nilsson SK, Haylock DN, Simmons PJ. Vascular cell adhesion molecule-1 (CD106) is cleaved by neutrophil proteases in the bone marrow following hematopoietic progenitor cell mobilization by granulocyte colony-stimulating factor. Blood 2001;98:1289–1297. [PubMed: 11520773]
28. Akiyama H, Chaboissier MC, Behringer RR, Rowitch DH, Schedl A, Epstein JA, de Crombrugghe B. Essential role of Sox9 in the pathway that controls formation of cardiac valves and septa. Proc Natl Acad Sci U S A 2004;101:6502–6507. [PubMed: 15096597]
29. Vidal VP, Chaboissier MC, Lutzkendorf S, Cotsarelis G, Mill P, Hui CC, Ortonne N, Ortonne JP, Schedl A. Sox9 is essential for outer root sheath differentiation and the formation of the hair stem cell compartment. Curr Biol 2005;15:1340–1351. [PubMed: 16085486]
30. Jackson LF, Qiu TH, Sunnarborg SW, Chang A, Zhang C, Patterson C, Lee DC. Defective valvulogenesis in HB-EGF and TACE-null mice is associated with aberrant BMP signaling. Embo J 2003;22:2704–2716. [PubMed: 12773386]
31. Miettinen PJ, Berger JE, Meneses J, Phung Y, Pedersen RA, Werb Z, Derynck R. Epithelial immaturity and multiorgan failure in mice lacking epidermal growth factor receptor. Nature 1995;376:337–341. [PubMed: 7630400]
32. Threadgill DW, Dlugosz AA, Hansen LA, Tennenbaum T, Lichti U, Yee D, LaMantia C, Mourton T, Herrup K, Harris RC, et al. Targeted disruption of mouse EGF receptor: effect of genetic background on mutant phenotype. Science 1995;269:230–234. [PubMed: 7618084]
33. Sibilia M, Wagner EF. Strain-dependent epithelial defects in mice lacking the EGF receptor. Science 1995;269:234–238. [PubMed: 7618085]
34. Pasparakis M, Alexopoulou L, Episkopou V, Kollias G. Immune and inflammatory responses in TNF alpha-deficient mice: a critical requirement for TNF alpha in the formation of primary B cell follicles, follicular dendritic cell networks and germinal centers, and in the maturation of the humoral immune response. J Exp Med 1996;184:1397–1411. [PubMed: 8879212]

35. Osawa M, Hanada K, Hamada H, Nakauchi H. Long-term lymphohematopoietic reconstitution by a single CD34-low/negative hematopoietic stem cell. Science 1996;273:242–245. [PubMed: 8662508]
36. Wilson A, Trumpp A. Bone-marrow haematopoietic-stem-cell niches. Nat Rev Immunol 2006;6:93–106. [PubMed: 16491134]
37. Li Z, Li L. Understanding hematopoietic stem-cell microenvironments. Trends Biochem Sci 2006;31:589–595. [PubMed: 16911868]
38. Adams GB, Scadden DT. The hematopoietic stem cell in its place. Nat Immunol 2006;7:333–337. [PubMed: 16550195]
39. Teitelbaum SL, Ross FP. Genetic regulation of osteoclast development and function. Nat Rev Genet 2003;4:638–649. [PubMed: 12897775]
40. Hirbe AC, Uluckan O, Morgan EA, Eagleton MC, Prior JL, Piwnica-Worms D, Trinkaus K, Apicelli A, Weilbaecher K. Granulocyte colony-stimulating factor enhances bone tumor growth in mice in an osteoclast-dependent manner. Blood 2007;109:3424–3431. [PubMed: 17192391]
41. Takahashi T, Wada T, Mori M, Kokai Y, Ishii S. Overexpression of the granulocyte colony-stimulating factor gene leads to osteoporosis in mice. Lab Invest 1996;74:827–834. [PubMed: 8606492]
42. Petit I, Szyper-Kravitz M, Nagler A, Lahav M, Peled A, Habler L, Ponomaryov T, Taichman RS, Arenzana-Seisdedos F, Fujii N, Sandbank J, Zipori D, Lapidot T. G-CSF induces stem cell mobilization by decreasing bone marrow SDF-1 and up-regulating CXCR4. Nat Immunol 2002;3:687–694. [PubMed: 12068293]
43. Kollet O, Dar A, Shivtiel S, Kalinkovich A, Lapid K, Sztainberg Y, Tesio M, Samstein RM, Goichberg P, Spiegel A, Elson A, Lapidot T. Osteoclasts degrade endosteal components and promote mobilization of hematopoietic progenitor cells. Nat Med 2006;12:657–664. [PubMed: 16715089]
44. Heissig B, Hattori K, Dias S, Friedrich M, Ferris B, Hackett NR, Crystal RG, Besmer P, Lyden D, Moore MA, Werb Z, Rafii S. Recruitment of stem and progenitor cells from the bone marrow niche requires MMP-9 mediated release of kit-ligand. Cell 2002;109:625–637. [PubMed: 12062105]
45. Forlow SB, Schurr JR, Kolls JK, Bagby GJ, Schwarzenberger PO, Ley K. Increased granulopoiesis through interleukin-17 and granulocyte colony-stimulating factor in leukocyte adhesion molecule-deficient mice. Blood 2001;98:3309–3314. [PubMed: 11719368]
46. Roberts AW. G-CSF: a key regulator of neutrophil production, but that's not all! Growth Factors 2005;23:33–41. [PubMed: 16019425]
47. Stark MA, Huo Y, Burcin TL, Morris MA, Olson TS, Ley K. Phagocytosis of apoptotic neutrophils regulates granulopoiesis via IL-23 and IL-17. Immunity 2005;22:285–294. [PubMed: 15780986]
48. Schwarzenberger P, Huang W, Ye P, Oliver P, Manuel M, Zhang Z, Bagby G, Nelson S, Kolls JK. Requirement of endogenous stem cell factor and granulocyte-colony-stimulating factor for IL-17-mediated granulopoiesis. J Immunol 2000;164:4783–4789. [PubMed: 10779785]
49. Kotake S, Udagawa N, Takahashi N, Matsuzaki K, Itoh K, Ishiyama S, Saito S, Inoue K, Kamatani N, Gillespie MT, Martin TJ, Suda T. IL-17 in synovial fluids from patients with rheumatoid arthritis is a potent stimulator of osteoclastogenesis. J Clin Invest 1999;103:1345–1352. [PubMed: 10225978]
50. Sibilia M, Wagner B, Hoebertz A, Elliott C, Marino S, Jochum W, Wagner EF. Mice humanised for the EGF receptor display hypomorphic phenotypes in skin, bone and heart. Development 2003;130:4515–4525. [PubMed: 12925580]
51. Sunnarborg SW, Hinkle CL, Stevenson M, Russell WE, Raska CS, Peschon JJ, Castner BJ, Gerhart MJ, Paxton RJ, Black RA, Lee DC. Tumor necrosis factor-alpha converting enzyme (TACE) regulates epidermal growth factor receptor ligand availability. J Biol Chem 2002;277:12838–12845. [PubMed: 11823465]
52. Sahin U, Blobel CP. Ectodomain shedding of the EGF-receptor ligand epigen is mediated by ADAM17. FEBS Lett 2007;581:41–44. [PubMed: 17169360]

53. Yamada T, Kaneko H, Iizuka K, Matsubayashi Y, Kokai Y, Fujimoto J. Elevation of lymphocyte and hematopoietic stem cell numbers in mice transgenic for human granulocyte CSF. Lab Invest 1996;74:384–394. [PubMed: 8780158]

54. Serizawa I, Amano K, Ishii H, Ichikawa T, Kusaka M, Taguchi T, Kiyokawa N, Fujimoto J. Long-term overexpression of human granulocyte colony-stimulating factor in transgenic mice: persistent neutrophilia with no increased mortality for more than one year. Cytokine 2000;12:630–635. [PubMed: 10843738]

55. Robinson SN V, Pisarev M, Chavez JM, Singh RK, Talmadge JE. Use of matrix metalloproteinase (MMP)-9 knockout mice demonstrates that MMP-9 activity is not absolutely required for G-CSF or Flt-3 ligand-induced hematopoietic progenitor cell mobilization or engraftment. Stem Cells 2003;21:417–427. [PubMed: 12832695]

56. Levesque JP, Liu F, Simmons PJ, Betsuyaku T, Senior RM, Pham C, Link DC. Characterization of hematopoietic progenitor mobilization in protease-deficient mice. Blood 2004;104:65–72. [PubMed: 15010367]

57. Brannan CI, Lyman SD, Williams DE, Eisenman J, Anderson DM, Cosman D, Bedell MA, Jenkins NA, Copeland NG. Steel-Dickie mutation encodes a c-kit ligand lacking transmembrane and cytoplasmic domains. Proc Natl Acad Sci U S A 1991;88:4671–4674. [PubMed: 1711207]

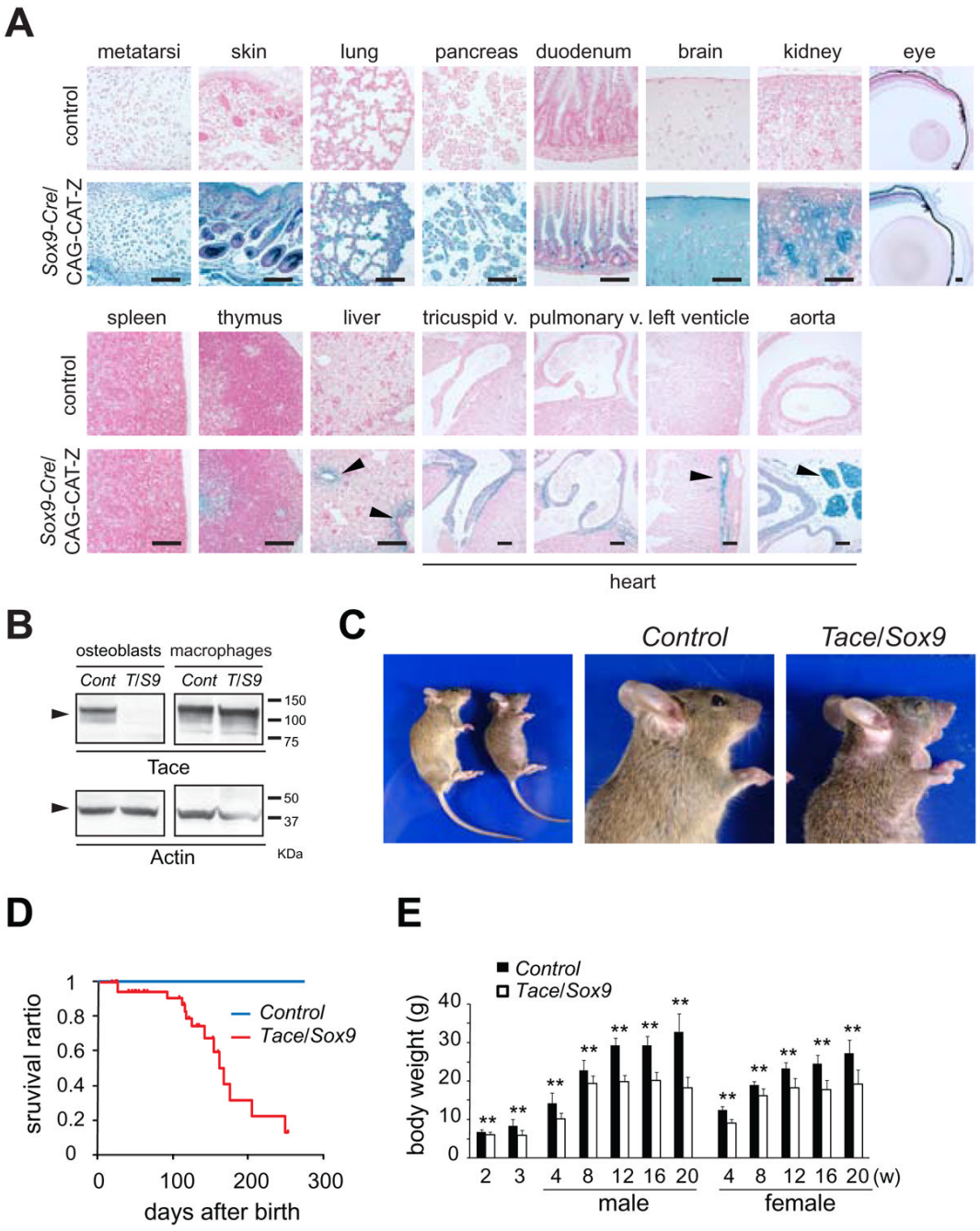

Figure 1.

Expression of *Sox9-Cre* and analysis of *Tace/Sox9* mice. (A) Analysis of the expression pattern of SOX9. Sections of various organs from *Sox9-Cre*/CAG-CAT-Z reporter mice stained with X-gal. Bars, 100 μm. β-gal positive cells are ubiquitously found in the growth plate (metatarsi), skin, lung, pancreas, intestine (duodenum), central nervous system (brain), kidney and eye. On the other hand, very little positive staining was found in the spleen, thymus or liver (except for the bile ducts and hepatocytes adjacent to the portal tracts in the liver as indicated by arrowheads). Heart sections revealed positive staining in the heart valves, coronary arteries and fat tissue (arrowheads). (B) Western blotting analysis of TACE in primary osteoblasts and bone marrow macrophages derived from *Control* (*Cont*) or *Tace/*

Sox9 (*T/S9*) mice. (C) Gross morphology of *Tace/Sox9* mice at 8 weeks after birth. Note that the *Tace/Sox9* mice have short hair and their eye lids remain closed. (D) Survival curve of *Control* and *Tace/Sox9* mice. (E) Weight of *Control* and *Tace/Sox9* mice at different postnatal ages (n = 5–30 for each genotype). Note that the weight of *Tace/Sox9* mice was approximately 15–20% less than that of *Control* mice up to 8 weeks of age; however these mice gain little weight after 8–12 weeks of age. **, $p < 0.005$.

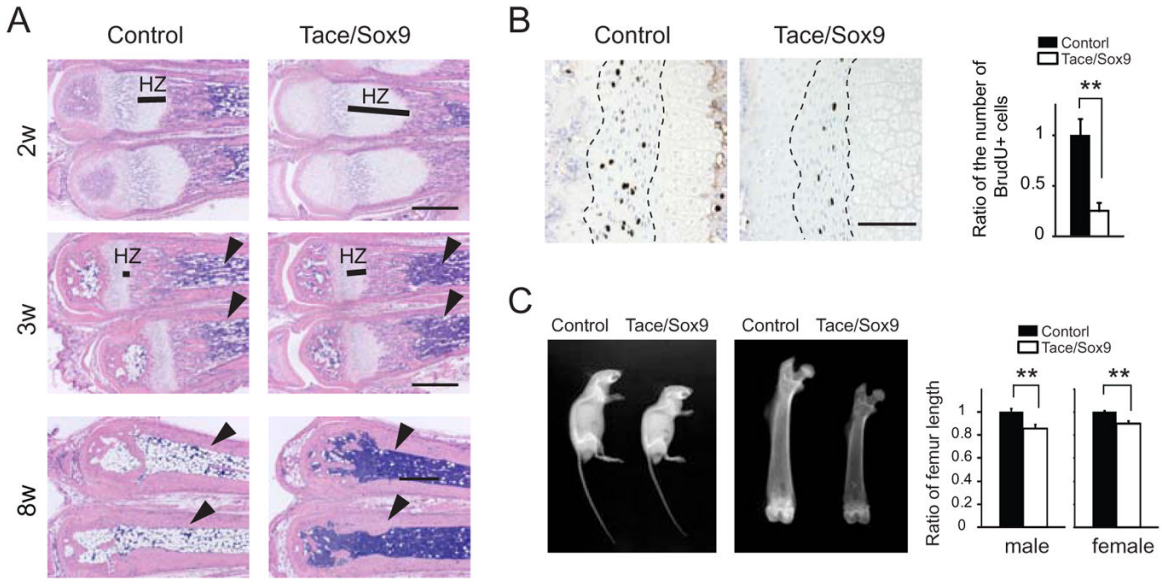

Figure 2.

Bone defects in *Tace/Sox9* mice. (A) Sections of metatarsi from 2, 3 and 8 week-old *Control* mice or *Tace/Sox9* mice. Note that *Tace/Sox9* bone marrow is not replaced with adipose tissue (3w and 8w, arrowheads). HZ, hypertrophic zone; bars, 500 μm. (B) Decreased chondroblast proliferation in *Tace/Sox9* mice. Immunolocalization of BrdU incorporation in the metatarsi. Bars, 100 μm. Ratio of the number of BrdU positive chondroblasts in the proliferating zone (outlined by broken lines) between *Control* and *Tace/Sox9* mice (right panel). The average of the number of BrdU positive cells from four *Control* mouse sections is set as 1. $n = 4$; **, $p < 0.005$. (C) Shorter length and lower bone mass in femurs from *Tace/Sox9* mice. Whole body X-ray analysis of 8 week-old male mice revealed no overt abnormality in the skeletal system (left panel). X-ray analysis of the femurs of 8 week-old mice (middle panel). The ratio of the length of the femur in *Control* and *Tace/Sox9* mice (right panel). The average length of *Control* is set to 1 ($n = 5$ for each genotype; male *Tace/Sox9* mice, 0.86 ± 0.031; female *Tace/Sox9* mice, 0.90 ± 0.026; **, $p < 0.005$).

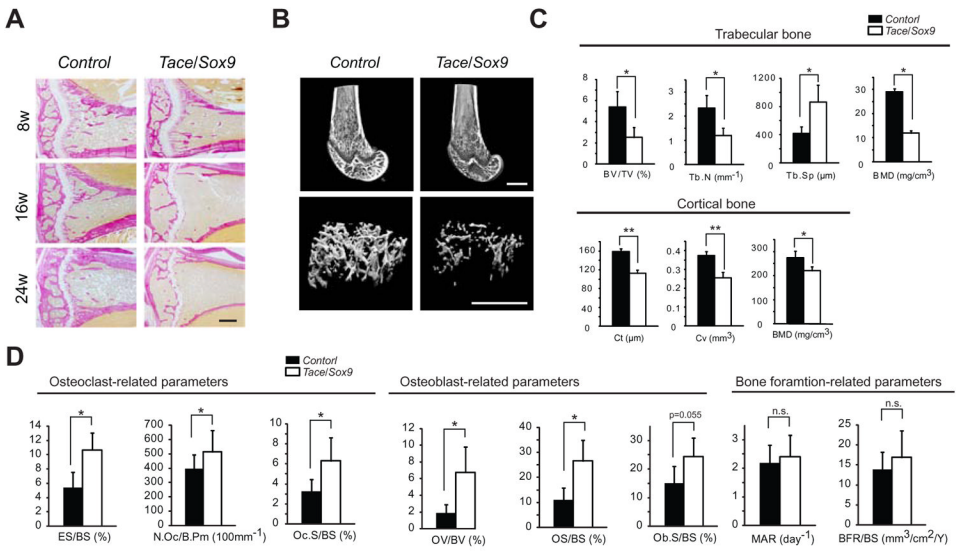

Figure 3.

Tace/Sox9 mice develop an osteoporosis-like phenotype. (A) van Gieson-stained sections of the tibias from 8, 16 and 24 week-old mice. Bars, 250 μm. (B) Reconstructed 3D images of microcomputed tomography of the distal femur of 8 week-old mice. Bars, 1 mm. (C) Microcomputed tomography analysis of the femur from 8 week-old *Control* and *Tace/Sox9* mice. BV/TV, bone volume/total volume; Tb.N, Tb.Sp, trabecular separation; BMD, bone mineral density; Cv, cortical volume; Ct, cortical thickness; *, $p < 0.05$; **, $p < 0.005$; n.s., not significant; $n = 4$ for each genotype. (D) Histomorphometric analysis of the femur from 8 week-old *Control* and *Tace/Sox9* mice. ES/BS, eroded surface/bone surface; N.Oc/B.Pm, osteoclast numbers/osteoclast perimeter; Oc.S/BS, osteoclast surface/bone surface; OV/BV, osteoid volume/bone volume; OS/BS, osteoid surface/bone surface; Ob.S/BS, osteoblast surface/bone surface; MAR, mineral apposition rate; BFR/BS, bone formation rate, surface referent; *, $p < 0.05$; n.s., not significant; $n = 4$ for each genotype.

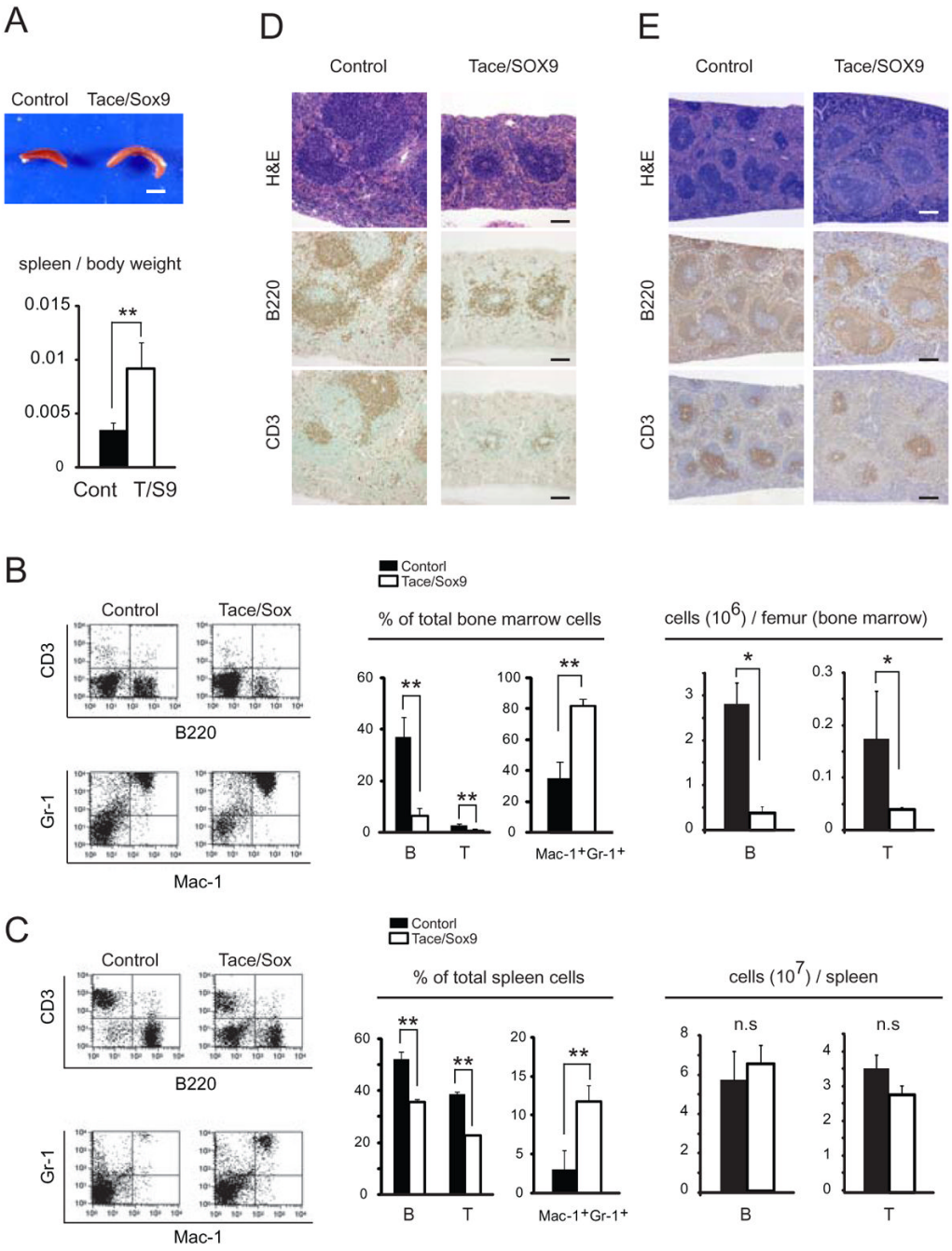

Figure 4.

Tace/Sox9 mice develop splenomegaly. (A) Gross appearance of the spleen from 8 week-old mice (upper panel; bar, 5 mm) and the spleen/body weight ratio. $n = 3$; **, $p < 0.005$. (B and C) Altered lymphocyte development and an increase in the population of Mac-1^+ Gr-1^+ cells in *Tace/Sox9* mice. The cells collected from bone marrow (B) and spleen (C) were double-stained for either CD3 and B220, or Gr-1 and Mac-1. B, $CD3^-$ $B220^+$ lymphocytes; T, $CD3^+$ $B220^-$ lymphocytes; $n = 3$; *, $p < 0.05$; **, $p < 0.005$; n.s., not significant. FACS analysis shown here is a representative result from three independent experiments. (D and E) Spleen sections from 3 week-old mice (D) and 8 week-old mice (E) stained with H&E, or

immunostained with anti-B220 or anti-CD3 antibody. Bars, 100 μm (D) and 250 μm (E), respectively.

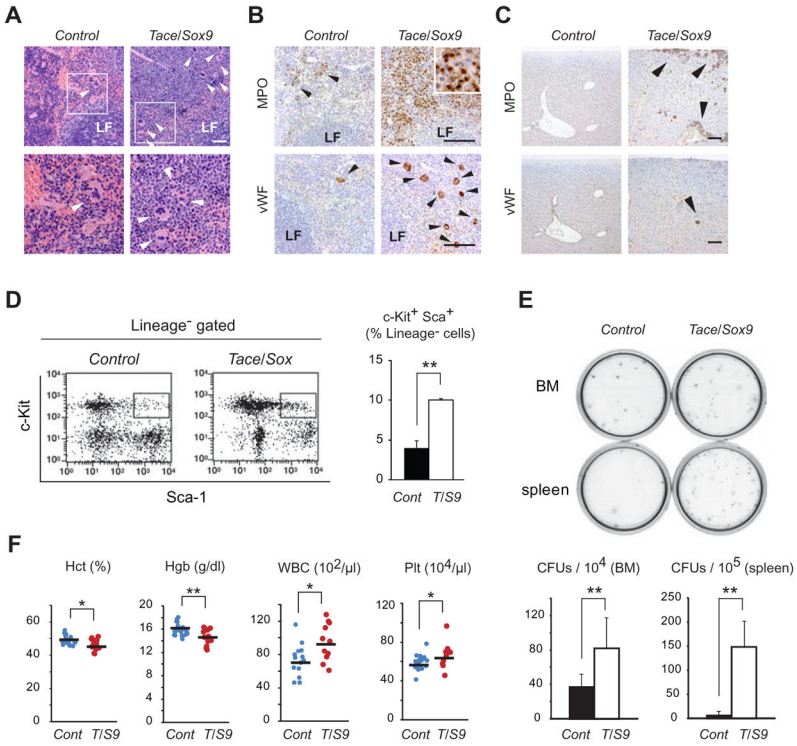

Figure 5.

Extramedullary hematopoiesis and increased KSL cell population in *Tace/Sox9* mice. (A) Histological analysis of a spleen from 16 week-old *Control* and *Tace/Sox9* mice. The sections are stained with H&E. Lower panels represent the boxed area in the upper panels. Note that many megakaryocytes are found in *Tace/Sox9* mice but few in *Control* (arrowheads). Bars, 50 μm. Sections of spleen (B) and liver (C) of a 10 week-old mouse are stained with anti-myeloperoxidase (MPO) or anti-von Willebrand factor (vWF). In the *Tace/Sox9* spleen, the red pulp is markedly expanded and is filled with numerous granulocytic cells of various differentiation stages which are strongly positive for MPO (inset). Increases in the number of megakaryocytes (arrowheads), which are positive for vWF, are also found in the red pulps. Similarly, MPO-positive myeloid cells and vWF-positive megakaryocytes are found in the liver of *Tace/Sox9* mice, but not of *Control* mice (arrowheads). LF, lymphoid follicles; bars, 100 μm. (D) An increase in KSL cell population in *Tace/Sox9* mice bone marrow. Boxed area indicates KSL cells. $n = 3$; *Control* (*Cont*), 4.0% ± 1.0; *Tace/Sox9* (*T/S9*), 10% ± 0.1. FACS analysis shown here is a representative result from three independent experiments. (E) Methylcellulose plates from day 10 of culture. Number of day 7 CFUs per 10^4 bone marrow cells (BM) and 10^5 splenocytes, respectively. $n = 3$; **, $p < 0.005$. (F) Complete blood counts of 8 week-old *Control* and *Tace/Sox9* mice. n=16; *, $p < 0.05$; **, $p < 0.005$.

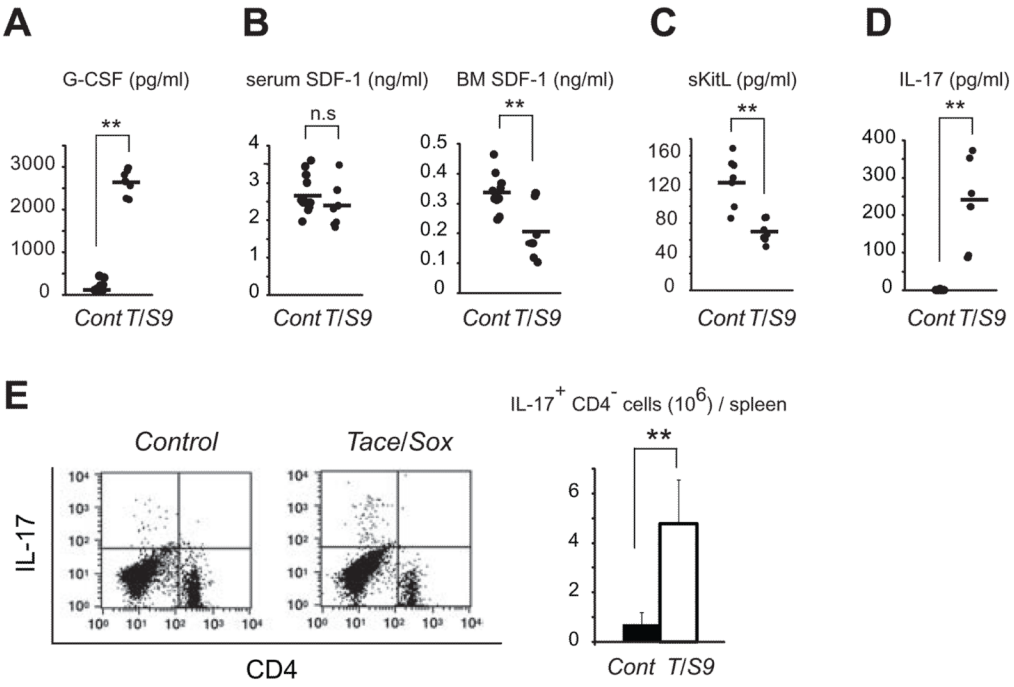

Figure 6.

Dysregulated production of G-CSF and IL-17 in *Tace/Sox9* mice. Analysis of serum G-CSF (A), serum and bone marrow (BM) SDF-1 (B), serum sKitL (C) and serum IL-17 (D) levels in *Tace/Sox9* (T/S9) or *Control* (Cont) mice by ELISA. (E) An increase in IL-17 producing cells in *Tace/Sox9* mice. $n = 3$. FACS analysis shown here is a representative result from three independent experiments. **, $P < 0.005$; n.s., not significant.